Planta (2008) 227:1351–1361
DOI 10.1007/s00425-008-0707-3

ORIGINAL ARTICLE

Fruit ripening in *Vitis vinifera*: apoplastic solute accumulation accounts for pre-veraison turgor loss in berries

Hiroshi Wada · Ken A. Shackel · Mark A. Matthews

Received: 15 December 2007 / Accepted: 4 February 2008 / Published online: 4 March 2008

Abstract In *Vitis vinifera* L. berries, the onset of ripening (known as "veraison") involves loss of turgor (P) in the mesocarp cells. We hypothesized that P loss was associated with an accumulation of apoplastic solutes in mesocarp tissue prior to veraison. Apoplastic sap was extracted from the mesocarp by centrifugation at the appropriate gravity to measure the apoplast solute potential (Ψ_s^A) and assay the sap composition. The Ψ_s^A was about −0.2 MPa early in development, decreased about 1.0 MPa by veraison, and continued to decrease during ripening to almost −4.0 MPa by the end of berry development. Potassium, malate, tartrate, proline, glucose, fructose, and sucrose were quantified in apoplastic sap. The calculated contribution of these solutes was about 50% of the total Ψ_s^A preveraison, but increased to about 75% as fructose and glucose accumulated during ripening. The contribution of the estimated matric potential to apoplast water potential decreased during development and was only 1.5% postveraison. We conclude that high concentrations of solutes accumulated in the mesocarp apoplast prior to veraison, and that P loss was a direct result of decreased Ψ_s^A. Because Ψ_s^A decreased before veraison, our findings suggest that apoplast solutes play an important role in the events of cellular metabolism that lead to the onset of ripening.

H. Wada · M. A. Matthews (✉)
Department of Viticulture and Enology, University of California, One Shields Ave, Davis, CA 95616-86383, USA
e-mail: mamatthews@ucdavis.edu

H. Wada
e-mail: hwada@ucdavis.edu

K. A. Shackel
Department of Plant Sciences/Pomology, University of California, Davis, CA, USA

Keywords Apoplast · Symplast · Grape · Turgor · Cell pressure probe · Centrifugation · Capillary electrophoresis · Symplast contamination · Veraison

Abbreviations

F	Firmness
P	Turgor
PostV	Postveraison
PreV	Preveraison
Ψ_m	Matric potential
Ψ_s	Solute potential
Ψ_s^A	Apoplast solute potential
Ψ_s^P	Protoplast (symplast) solute potential
Ψ_s^T	Tissue solute potential
Ψ_w	Total water potential
Ψ_w^A	Apoplast total water potential
Ψ_w^P	Protoplast (symplast) total water potential

Introduction

Most fleshy fruits accumulate high concentrations of solutes (mainly sugars) in the cells during fruit development (Coombe 1976). Grape berries, which accumulate high concentrations of hexoses during ripening, are representative of nonclimacteric fruit that exhibit a dynamic, double sigmoid growth habit. The two periods of growth, Stage I and Stage III, are separated by a period of little or no fruit expansion, Stage II. The onset of ripening (known as "veraison") occurs at the transition from Stage II to Stage III. Fruit development typically includes the genetically programmed process of softening during ripening. The mechanism for this softening process has been extensively

studied, although most of the work concerning the molecular basis of fruit softening has focused on the altered metabolism of the cell wall/middle lamella complex (Wakabayashi 2000; Brummell and Harpster 2001) and the changes in cell wall-related gene expression that occur during the ripening process (e.g., Rose et al. 1997; Hiwasa et al. 2004). Another important factor, however, is the water relations of cells and tissues (Saladié et al. 2007), and the expected dependence of tissue mechanical properties on cell turgor (P) (Bruce 2003).

Recently, Matthews and Shackel (2005) and Thomas et al. (2006), showed that mesocarp cell P decreases at or near veraison, when berries soften (Coombe and Bishop 1980). A positive correlation between fruit Firmness and fruit cell P has been observed in tomato (Mignani et al. 1995) and harvested apple fruits (Tong et al. 1999). These observations suggest an important contribution of P to fruit softening and perhaps to ripening. For instance, P loss preceded skin reddening and wall carbohydrate composition changes in tomato (Shackel et al. 1991). Given the high concentration of solutes present in ripening berries (Matthews et al. 1987; Tyerman et al. 2004), Matthews and Shackel (2005), speculated that apoplastic solutes play an important role in preventing the occurrence of excessive P in berries as part of normal development, presumably to reduce the risk of cracking/splitting which may be caused by a sudden increase in plant and soil water availability (Considine and Brown 1981).

Apoplast sap has been extracted from plant organs with several techniques: (1) the pressure chamber technique (Boyer 1967; Jachetta et al. 1986; Nonami and Boyer 1987; Tang and Boyer 2002; Wada et al. 2005), (2) the vacuum perfusion technique (Bernstein 1971; Cosgrove and Cleland 1983), and (3) the centrifugation technique (with and without infiltration) (Terry and Bonner 1980; Cosgrove and Cleland 1983; Meinzer and Moore 1988; Welbaum and Meinzer 1990; Speer and Kaiser 1991; Tetlow and Farrar 1993; Dannel et al. 1995; Pomper and Breen 1995; Zhang et al. 1996; Livingston and Henson 1998; Lohaus et al. 2001; Zhu et al. 2006). Of these, the centrifugation technique is the most common. In centrifuge studies with vacuum infiltration, dilution and other artifactual changes of apoplast solute concentrations are concerns (Lohaus et al. 2001). Therefore, we adopted a centrifuge technique without infiltration according to Welbaum and Meinzer (1990) and Pomper and Breen (1995), in which we determined an appropriate centrifugal force for each stage of berry development. In this work, we demonstrate the importance of berry apoplastic solutes to fruit cell P by combining apoplast extraction techniques and in situ P measurements. The magnitude of symplast contamination in apoplast sap during the extraction is also considered.

Materials and methods

Plant materials

Two-year-old grapevines (*Vitis vinifera* L. cv. Chardonnay) were grown from dormancy in 5-L pots filled with a mixture of GrowCoir^{TM} (Greenfire Co., Ltd., Sacramento, CA, USA), clay pellets, and perlite (4:1:1 by volume) in a greenhouse (30/20 ± 3°C; 40/70 ± 10% RH; and natural light with a daily maximum of 1,200 μmol photons m^{-2} s^{-1} PAR). The vines were pruned to two shoots with one or two clusters per shoot, and the shoots were vertically trained to approximately 1.5 m. Vines were fully watered daily with a modified Hoagland's nutrient solution (in mM: NO_3^-, 6.85; NH_4^+, 0.43; PO_4^{3-}, 0.84; K^+, 3.171; Ca^{2+}, 2.25; Mg^{2+}, 0.99; SO_4^{2-}, 0.50; and in μM: Fe^{2+}, 28.65; Mn^{2+}, 4.91; BO_3^{3-}, 24.05; Zn^{2+}, 1.83; MoO_4^{2-}, 0.17; Cu^{2+}, 2.52) with EC 1.00 dS m^{-1} at pH 5.75. The water potential of nutrient solution was −0.04 ± 0.01 MPa. The anthesis date was noted as the day in which 50% of the cluster was flowering. All flowering within a cluster occurred within 2–3 days. Veraison was defined by inspection as a marked inflection point of the curve of soluble solids over time. Berries at various days after anthesis (DAA) were selected from different parts of the cluster, excised at the pedicel, and immediately placed into aluminized mylar bags that excluded light and prevented transpiration.

Assaying turgor

The cell pressure probe technique (Hüsken et al. 1978) modified as described previously (Shackel et al. 1987) was used to measure the P of individual cells in the berry mesocarp between depths of 100–1,000 μm from the epidermis according to the procedure of Thomas et al. (2006). Briefly, microcapillary tips were prepared by a Koph 750-micropipette puller and were beveled in a jetstream of beveling solution (Ogden et al. 1978) modified as described previously (Shackel et al. 1987). Micropipettes were inserted perpendicularly to the surface along the equatorial plane of the berries. All measurements were performed under laboratory conditions (diffuse fluorescent light, 25°C air temperature, and localized 100% RH obtained with a humidifier) and were generally completed within 12 h of detachment from the cluster depending on the sample size. Previous work has shown that the berry P does not change significantly for up to 48 h after being excised from the vine if water loss from the berry is prevented (Thomas et al. 2006).

Extraction of apoplast and tissue sap

Each berry was cut with a razor blade, removing approximately 2 mm of the pericarp (referred to as 'residual') at

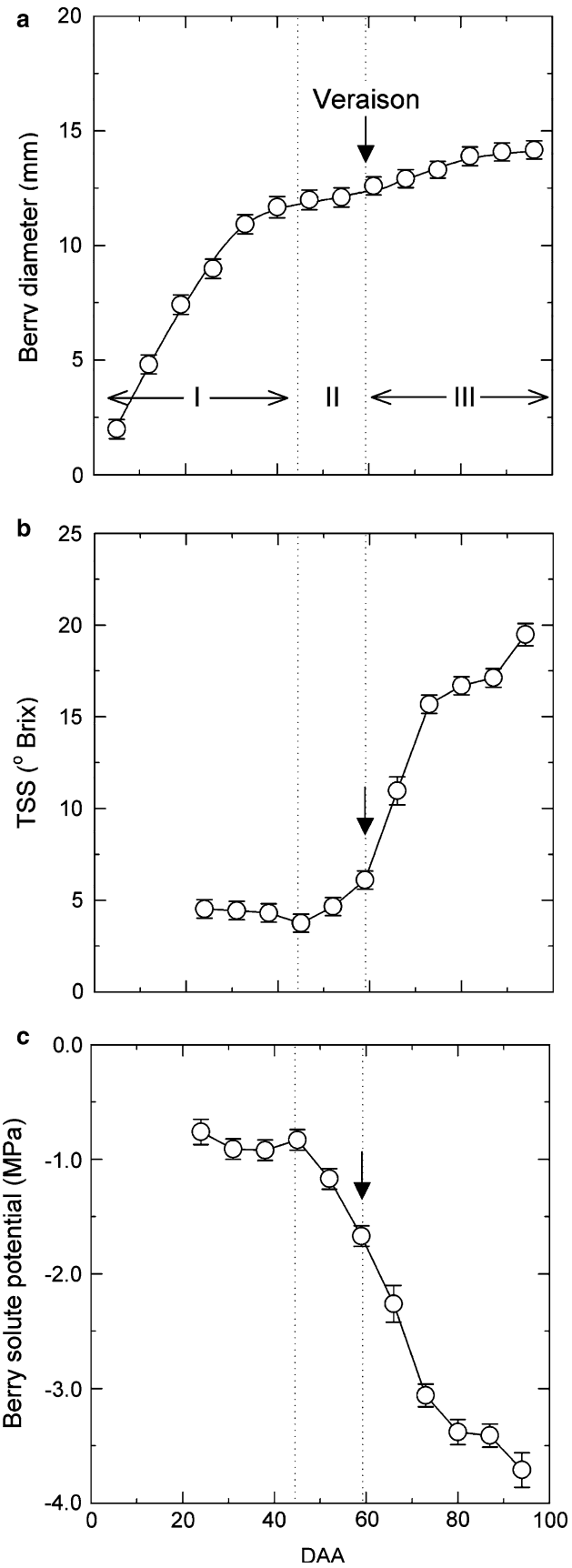

Fig. 1 Diameter (**a**), total soluble solids (TSS, °Brix, **b**) and berry solute potential (**c**) of individual berries sampled from greenhouse-grown Chardonnay vines at various days after anthesis (DAA). The data were taken during two growing seasons, with anthesis on May 18, 2005 (**a**), and February 26, 2005 (**b**, **c**). Data are Mean ± SE ($n = 3$–13). The *two dotted lines* indicate the estimated borders of the three developmental stages, Stage I, Stage II, and Stage III and the *arrows* indicate the growth transition between Stage II and Stage III (as "veraison"), which was estimated based on the rate of soluble solids increase (see Results)

the stylar (distal) end of the berry (see inset of Fig. 2). The flat cut surface of the berry was carefully blotted with Kimwipe (except where this factor was being tested) and immediately placed on a circular support screen set at 35 mm from the bottom of a 12-mL glass centrifuge tube. The top of the tube was sealed entirely with paraffin film to prevent water loss from the samples. Samples were centrifuged in the range of 100–1,500×g for 20 min at 4°C, and extracted sap was collected from the bottom of the centrifuge tube. The extraction was completed within 1–4 h after harvest.

In a preliminary experiment, three procedures for handling the cut surface, no blotting, blotting, washing/blotting (blotting immediately after rinsing with distilled water for 1 s) were compared for their effects on volume of sap obtained and apparent apoplast solute potential (Ψ_s^A). A sample of six to eight berries in preveraison (PreV) and in postveraison (PostV) was randomly assigned to one of the three blotting treatments prior to extraction. For the volume of sap obtained, one-way ANOVA and Duncan's multiple range tests were used to compare treatment means within each stage of berry development. For Ψ_s^A, treatment least-squares means were compared using tissue solute potential (Ψ_s^T) as a covariate within each stage (significant for each stage at $P < 0.01$; ANCOVA not shown).

Solute potential measurements

Both the Ψ_s^A and Ψ_s^T were determined using dewpoint osmometry (5500 vapor pressure osmometer, Wescor Inc.). For apoplastic sap, the Ψ_s^A was determined immediately after centrifugation. When the sample volume was less than 5 μL, two or more samples were pooled. For Ψ_s^T from mesocarp tissue, the residual (non-centrifuged) and centrifuged tissues were immediately frozen at −90°C for 2 h and stored at −20°C. The Ψ_s^T from the residual and the centrifuged tissues was measured with the supernatant of fluid sap obtained by centrifuging at 2,000×g for 10 min after thawing at 25°C. For some berries, the sap was extracted by squeezing after freezing and thawing the entire berry to determine the solute potential (Ψ_s). In this case, we refer to berry Ψ_s (see Fig. 1).

Sap pH

The pH of apoplast sap (>5 μL) and of corresponding tissue sap (from residual tissue) was measured with the Ultra-M micro pH electrode (PHR-146S, Lazar Research Laboratories, Inc., Los Angeles, CA, USA) and MI-410 Combination pH electrode (Microelectrodes, Inc., Bedford, NH, USA) under controlled temperature conditions.

Solute composition of apoplastic and tissue sap

The solute composition in apoplast and tissue sap (2–4 μL of sap solution) was identified and quantified using an Agilent capillary electrophoresis (CE) system (G1600AX, Agilent Technologies, Germany). The CE analysis was performed according to Soga and Imaizumi (2001). Separations were carried out on fused silica capillaries with 50 μm i.d. × 112.5 cm total length (104 cm effective length). Before each injection, the capillary was preconditioned for 5 min by flushing with Agilent basic anion buffer, which was used as the run buffer. The sample was injected with a pressure of 50 mbar for 6.0 s. The applied voltage was set at −30 kV and the capillary temperature was thermostatted to 15°C. Detection wavelength was set at 350 nm for constant signal wavelength and at 230 nm for reference wavelength. Unknown peaks were identified by co-electropherogram with internal standard solutes. The concentration of tartrate, malate, proline, fructose, glucose, and sucrose was quantified. The soluble potassium concentration was determined by atomic absorption spectrometry.

For comparison to the measured Ψ_s^A, a predicted Ψ_s of the apoplastic sap could be calculated from the sum of concentrations of these measured solutes according to the van't Hoff relation,

$$\Psi_s = -RT\left(\frac{n_s}{V}\right) \quad (1)$$

where R, T, and n_s/V are the gas constant (8.32×10^{-6} MPa m^3 mol^{-1} K^{-1}), absolute temperature (K), and the molar concentrations (mol m^{-3}) of each solute, respectively.

Results

Berry growth and solute potential

Although the double-sigmoid pattern of berry enlargement was evident from berry diameter, it was difficult to discern the growth transition from Stage II to Stage III of individual berries for greenhouse-grown Chardonnay (Fig. 1a). Therefore, this transition, veraison was defined by the inflection point of the soluble solids curve over time as occurring at 59 DAA. The rate of soluble solids accumulation increased fourfold from DAA 45–59 to DAA 59–73 (0.17–0.68 °Brix day^{-1}, respectively, Fig. 1b). Berry solute potential (Ψ_s) ranged from −0.76 to −0.96 MPa during Stage I. Subsequently, berry Ψ_s decreased rapidly from Stage II to veraison, and then more slowly from the middle of Stage III (Fig. 1c). The early increase during Stage II of solutes was clearer in Ψ_s (Fig. 1c) than it was in soluble solids (Fig. 1b), presumably because osmomtery is more sensitive to total solutes than refractometry. Accordingly, Ψ_s measurement was conducted subsequently to monitor berry development.

Obtaining sap from tissue and apoplast

The volume of apoplastic sap obtained from Stage III berries was much larger (significant at $P < 0.03$; ANOVA not shown) than that obtained from Stage II berries, and within each stage, blotting generally reduced the volume of sap obtained compared to no blotting (Table 1). In the no-blot treatment, apparent apoplastic solute potential (Ψ_s^A) was similar to the tissue solute potential (Ψ_s^T) regardless of berry stage, presumably due to significant symplast contamination in the recovered sap (Table 1). For PreV berries, blotting significantly increased apparent Ψ_s^A,

Table 1 Effect of washing and/or blotting the berry cut surface prior to centrifugation on the collected sap volume, apoplast solute potential (Ψ_s^A) and tissue solute potential (Ψ_s^T) in three treatments

Treatments	PreV			PostV		
	Collected sap volume (μL)	Ψ_s^A (MPa)	Ψ_s^T (MPa)	Collected sap volume (μL)	Ψ_s^A (MPa)	Ψ_s^T (MPa)
No-blot	5.9 ± 5.4a	−0.90 ± 0.11b	−0.99 ± 0.11	52.5 ± 28.4a	−4.52 ± 0.36ab	−4.40 ± 0.33
Wash/Blot	2.2 ± 0.5b	−0.37 ± 0.05[1]a	−0.98 ± 0.06	20.9 ± 14.6b	−4.76 ± 0.32b	−4.37 ± 0.54
Blot	1.9 ± 0.5b	−0.44 ± 0.11[1]a	−1.03 ± 0.09	32.1 ± 12.7ab	−4.37 ± 0.38a	−4.50 ± 0.30

The sap from late Pre- and PostV berries was extracted by centrifugation at 410 and 100×g, respectively. Tissue sap was obtained from squeezing the tissues after freezing/thawing. Data indicate Mean ± 1 SD (n = 6–8). Statistical tests used for mean separations within each stage, were Duncan's multiple range for collected sap volume and pairwise comparison of LS means for Ψ_s^A (see text for details)

[1] More than two sap samples were pooled and the Ψ_s^A was measured (n = 3)

presumably due to removal of contaminating symplast solutes, but for PostV samples, blotting did not have a consistent effect on Ψ_s^A, and the values were always similar to that of Ψ_s^T (Table 1). Since blotting presumably removed surface contamination in PreV berries, and since washing presumably may cause inconsistent dilution of the Ψ_s^A, the blotting procedure prior to centrifugation was used in all subsequent experiments.

We tested whether centrifuge extraction per se affected Ψ_s^T by comparing the Ψ_s of centrifuged and non-centrifuged portions of the same berry. For samples (berries) taken at different stages of development, the regression line between the Ψ_s of sampled (x) and residual (non-centrifuged) tissues (y) was $y = 1.04x + 0.03$ with $r^2 = 0.99$, and the relationship was linear and essentially equivalent across a broad range of centrifuged tissue Ψ_s (−0.62 to −4.03 MPa) (Fig. 2). Based on this result, non-centrifuged tissue was measured as representative Ψ_s^T in the following measurements.

Determination of the appropriate centrifugal force

We determined an appropriate centrifugal force for sap extraction at each stage of development by evaluating the volume, Ψ_s^A, and pH of extracted sap for samples centrifuged at different gravities (100–1,500×g). In Stage I, the sap volume was small and always less than 10 μL even at a centrifugal force of 1,500×g (Fig. 3a). In Stage II, small and similar sap volumes were recovered up to 500×g, thereafter the sap volume increased with centrifugation force (Fig. 3b). In PostV, approximately 8 μL of sap was recovered at less than 175×g, but the volume increased substantially when more than 200×g was applied (Fig. 3c).

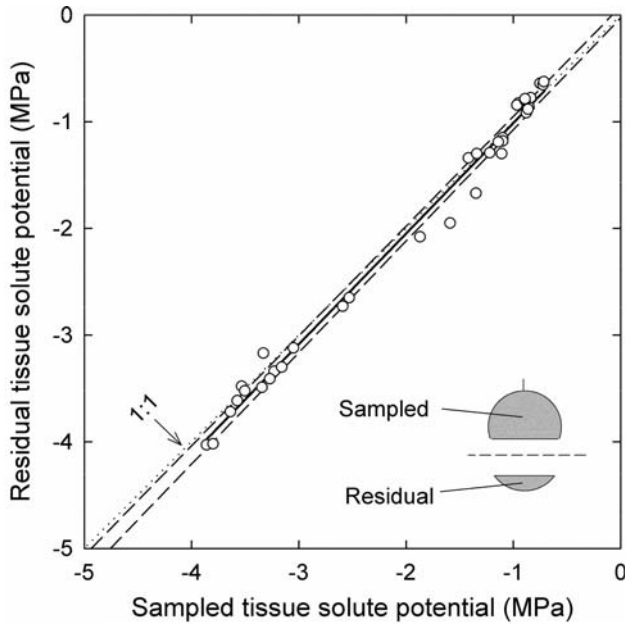

Fig. 2 Residual tissue solute potential as a function of sampled tissue solute potential from individual berries sampled from greenhouse-grown Chardonnay vines at various days after anthesis (*DAA*). The *solid line* indicates the regression line. Working–Hotelling hyperbolic confidence bands for the regression lines were calculated from data points at $P = 0.95$. Hyperbolic confidence curves for regression line are drawn with *dashed lines*. The *dotted line* indicates the equipotential line

At lower gravities, Ψ_s^A of PreV berries was unchanged, but as the force increased above 500×g Ψ_s^A decreased, and at 1,500×g approached Ψ_s^T (Fig. 3d, e). At low gravity, the Ψ_s difference between apoplast and tissue was high (approximately 0.65 MPa) and dramatically decreased as the force increased (Fig. 3g, h), suggesting that the lowering of Ψ_s^A might be due to symplast contamination by cell damage. In PostV berries, the Ψ_s^A was similar to Ψ_s^T throughout the range of 100–1,500×g. Thus, the Ψ_s difference in PostV berries was much smaller than in PreV berries even when the tissue was centrifuged at low gravity (Fig. 3i).

As a third test of symplast contamination, we measured the pH of apoplast and tissue sap solutions obtained under the same range of gravity. For all stages of development, the pH of apoplast sap collected at <500×g was approximately 4.0 and much higher than tissue pH (Fig. 4a–c). The pH of apoplastic sap collected at higher gravities decreased towards the tissue pH. From these observations, the appropriate centrifugal force of Pre- and Post-V berries for subsequent work was set at 350 and 100×g, respectively.

Apoplastic solutes increase during development

The Ψ_s^A decreased from the first sample date (30 DAA) throughout development. The Ψ_s^A began at −0.23 MPa at 30 DAA and reached −3.77 MPa at 95 DAA (Fig. 5a). The Ψ_s^A decreased approximately 1.0 MPa during Stage II, well prior to veraison. The Ψ_s^T was relatively stable during Stage I but clearly decreased after 42 DAA, from −0.75 to −3.74 MPa at 95 DAA. The difference between apoplast and tissue solute potential (Ψ_s^A–Ψ_s^T) should represent a reliable index of apoplastic solute accumulation because berry sample-to-sample variation is minimized. The Ψ_s^A–Ψ_s^T at 30 DAA was 0.52 MPa, diminished to 0.13 MPa prior to Stage II, and reached approximately zero at 78 DAA (Fig. 5b). This indicates a relatively greater solute accumulation in the apoplast than in tissue as a whole.

The decrease in PostV Ψ_s^A is closely associated with the accumulation of glucose and fructose in the apoplast

For Stage I, the concentration of each solute detected in apoplast sap (ranging from 0.66 to 13.7 mM) was lower than that of tissue sap, and the differences were significant

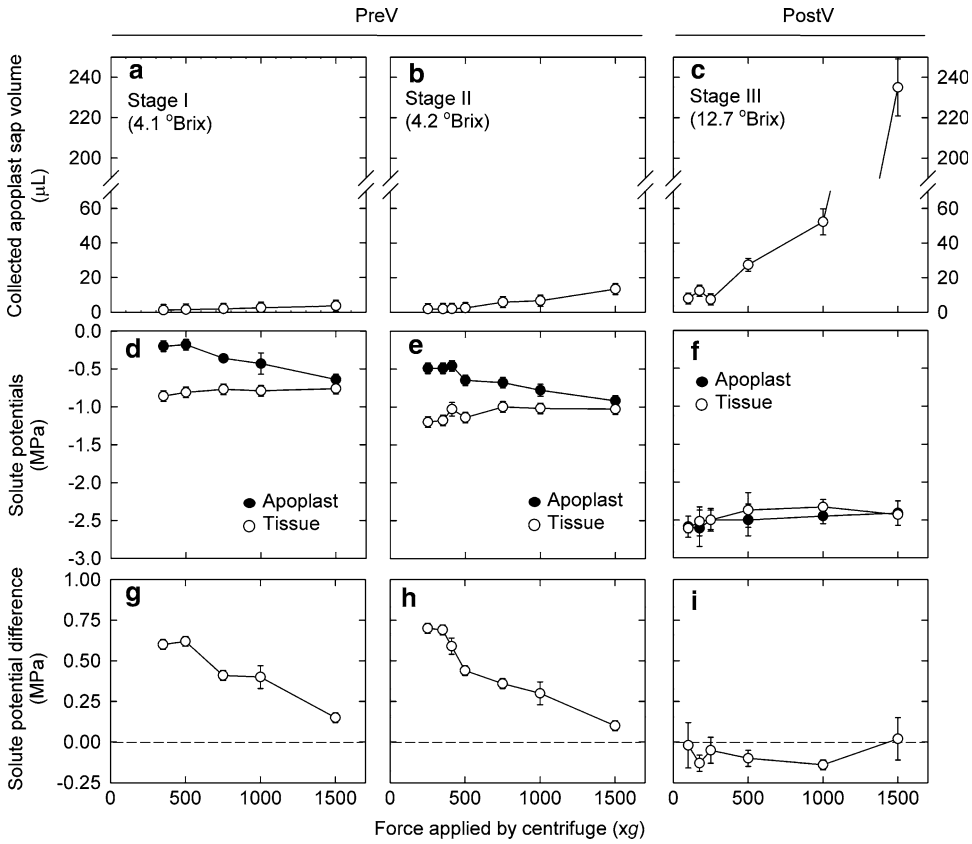

Fig. 3 Apoplast sap volume (**a, b, c**), apoplast (*closed circles*) and tissue (*open circles*) solute potential (**d, e, f**), and difference in solute potential (apoplast–tissue, **g, h, i**) as a function of force applied by the centrifuge at three different berry developmental stages (Stage I, Stage II, and Stage III). Average soluble solids are inserted in **a**–**c**. Data are Mean ± SE (n = 3–16) from individual berries sampled on 2–3 different sampling dates (from April 26, 2005 to May 24, 2005)

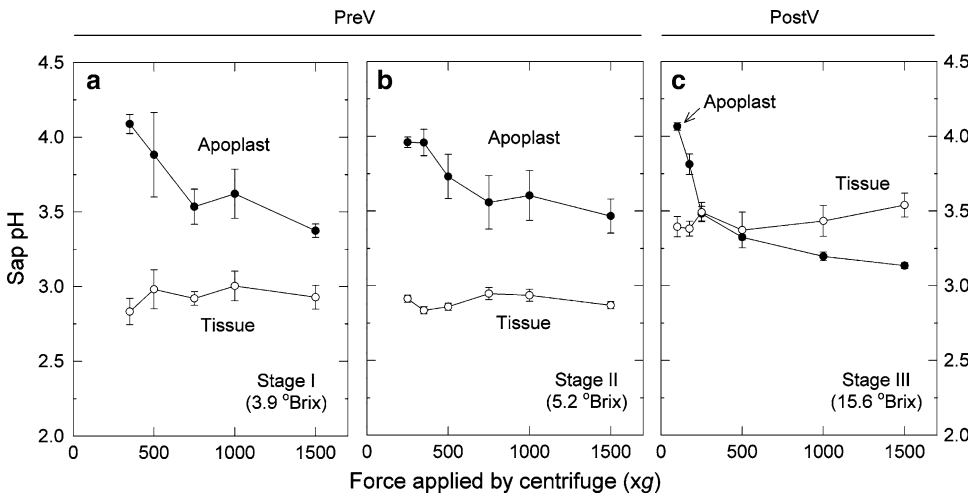

Fig. 4 Apoplast (*closed circles*) and tissue (*open circles*) pH as a function of force applied by the centrifuge at three different berry developmental stages. Averaged soluble solids are inserted. Data are Mean ± SE (n = 3–8) from individual berries sampled on 2–3 different sampling dates (from August 11, 2005 to January 26, 2006)

for malate and potassium (Fig. 6a). Hence, the summed solute concentration in apoplast sap was also significantly lower than that of tissue sap (Fig. 6a). From Stage I to Stage II, the concentration of malate increased in apoplast sap and in tissue sap, but the concentration of tartrate only increased in the apoplast sap (Fig. 6a, b). These increases along with increases in the concentrations of proline, fructose, glucose, and sucrose in apoplast sap caused the summed solute concentration to increase about threefold, to approximately 180 mM, similar to that of tissue (195 mM) (Fig. 6b). The PostV concentration of fructose (560 mM) and glucose (300 mM) in apoplast sap was much higher than that of Stage II, but the concentration of fructose was significantly lower than in the tissue (Fig. 6c). The summed concentration of these solutes in the apoplast reached 990 mM PostV (Fig. 6c), a further fivefold increase over Stage II.

As a consequence of the differences in solute concentrations, the contribution of specific solutes to the total solute potential also differed between apoplast and tissue

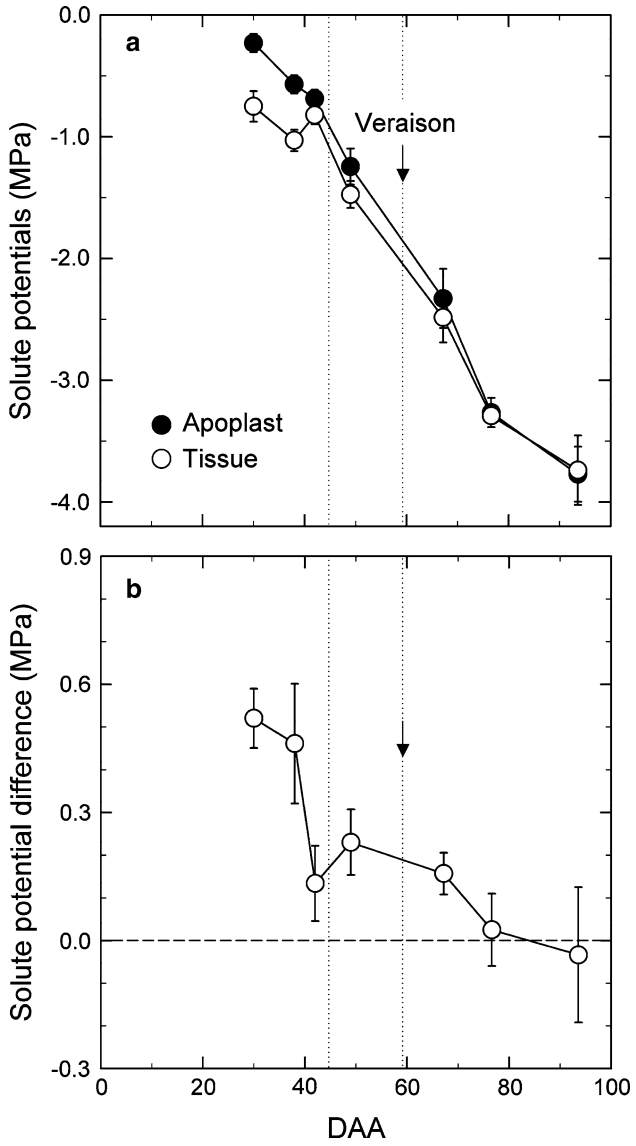

Fig. 5 Apoplast (**a**, *closed circles*), and tissue (**a**, *open circles*) solute potential and the difference in solute potential (apoplast–tissue, **b**) in greenhouse-grown Chardonnay berries over time (*DAA*). A centrifugal force of 350 and 100×*g* was used for apoplastic sap extraction of Pre- and PostV berries, respectively. The *two dotted lines* indicate the estimated borders of the three developmental stages, Stage I, Stage II, and Stage III, and the *arrows* indicate the growth transition between Stage II and Stage III (as "veraison"), which was estimated based on the rate of soluble solids increase (see Results). Data are Mean ± SE (n = 3–6) from individual berries sampled on 7 different DAA (from April 12, 2005 to June 8, 2005)

sap. For Stage I, malate contributed 17 and 4%, whereas fructose contributed 6 and 15% of the Ψ_s of tissue and apoplast sap, respectively (Fig. 6d). The primary change in Stage II was the increased contribution of malate to Ψ_s^A, and the contribution of proline also increased, although the contribution of potassium decreased (Fig. 6e). The primary change from Stage II to Stage III was that fructose and glucose became the dominant factors in both Ψ_s^A and Ψ_s^T (Fig. 6f). The calculated Ψ_s at Stage I, Stage II, and Stage III (−0.12, −0.45, and −2.55 MPa, respectively) is given with corresponding berry-soluble solids, P, Ψ_s^T, and the measured Ψ_s^A in Table 2.

Discussion

In this work, we hypothesized that significant concentrations of apoplastic solutes occur in ripening grape berries (as well as in other fruits that accumulate high amounts of sugars), and that the low Ψ_s of fruit apoplast sap contributes to the low PostV P that we recently reported (Matthews and Shackel 2005; Thomas et al. 2006). The results show that the composition and Ψ_s of fruit apoplast sap are dynamic during fruit development and that the concentration of apoplast solutes increased almost 1 M during development. Consequently, the Ψ_s^A decreased several MPa from Stage I, causing or contributing to a reduction in the Ψ_s difference between tissue (presumably, symplast) and apoplast in the mesocarp. In PostV berries, the Ψ_s^A reached −3.37 MPa, similar to the −3.48 MPa of the tissue, and mesocarp cell P was a correspondingly low 0.06 MPa. Hence, our results indicate that apoplastic solute accumulation is associated with P loss at the onset of ripening.

We carefully extracted apoplast sap from the berries with the low-speed centrifuge technique. By imposing neither infiltration nor perfusion, potential dilution and mixing artifacts (Welbaum and Meinzer 1990; Pomper and Breen 1995; Yu et al. 2000) were avoided. The additional critical issue for the centrifuge technique is potential symplastic contamination generated by cell damage. This concern is exacerbated by the suggestions that cell membrane degeneration and solute leakage from symplast to apoplast are integral to veraison (Lang and Thorpe 1989; Lang and Düring 1991). Therefore, we altered the centrifugal force applied to berries taking into account decreases that occur in Firmness and P during fruit development (data not shown, Thomas et al. 2004). We evaluated the magnitude of symplast contamination several ways including by measuring the changes in the volume yield, Ψ_s, and pH of apoplast sap solutions under the different centrifugal force at each developmental stage.

First, in PreV berries it was possible to find regions of centrifugal force to which the volume yield and Ψ_s differences (i.e., Ψ_s^A–Ψ_s^T) were similar. Above those regions, yield increased and (Ψ_s^A–Ψ_s^T) decreased significantly, presumably due to increasing cell damage. For volume yield from PostV berries, these regions were at considerably lower centrifugal forces than for PreV berries, but the Ψ_s^A was similar to Ψ_s^T even when the tissue was centrifuged at very low gravity (e.g., 100–250×*g*). Although the low PostV Ψ_s^A

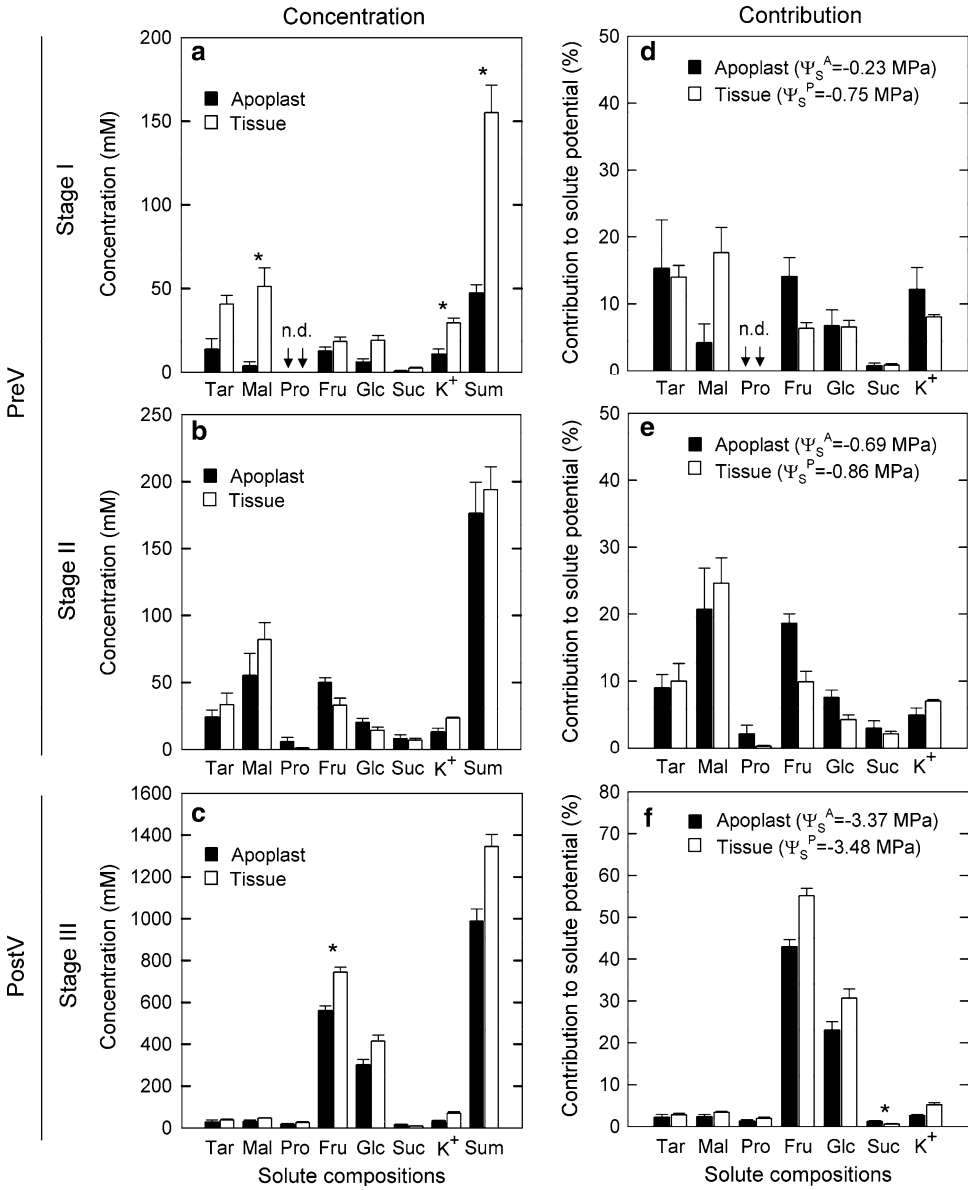

Fig. 6 Solute composition of tissue and apoplast sap assayed at three developmental stages (**a**–**c**) and the relative contribution to the respective calculated total solute potential (**d**–**f**). "Tar", "Mal", "Pro", "Fru", "Glc", "Suc", "K^+", and "Sum" indicate tartrate, malate, proline, fructose, glucose, sucrose, potassium, and summed solute concentration, respectively. The values of measured apoplast and tissue solute potential are inserted into **d**–**f** (see Table 1). 'n.d.' means not detected. Data are Mean ± SE (n = 3–6) from individual berries from 2 clusters sampled on October 18, 2005 for Stage I and June 28, 2005 for Stage II and Stage III, respectively. *Asterisk* indicates statistically significant difference (Student's t test, $P < 0.05$) between apoplast and tissue sap solutions

was probably due to a high concentration of apoplastic solutes, it is possible that there was sufficient symplast contamination in apoplastic sap from PostV berries to essentially equilibrate the Ψ_s^T and Ψ_s^A. We then measured apoplastic sap pH and compared it to tissue pH to discriminate the cause of the decreased Ψ_s^A. The low pH of the berry may reflect the higher concentration of organic acids in fruit than other organs such as leaf and root (Sakurai 1998). As soluble solids increase from 3.9 to 15.6 °Brix, the pH of tissue sap increases from 2.9 to 3.5 (Matthews and Anderson 1988; Gutiérrez-Granda and Morrison 1992; Tyerman et al. 2004), and that is what we observed (Fig. 4). In contrast, the pH of apoplast sap is higher than that of berry tissue (presumably symplast) sap, which is consistent with the observation by Welbaum and Meinzer (1990). When samples were obtained at higher centrifugal forces, the pH of the apoplast moved towards the tissue pH, again consistent with increasing cell damage only at high centrifuge speeds. Although the composition of apoplast and tissue samples were similar in general (based upon the few solutes analyzed), there were several important differences in addition to pH. The sap composition of PreV berries, in which the concentration of tartrate, malate, and K^+ were significantly lower in apoplast sap than in tissue sap, demonstrates that two distinct pools were sampled. Thereafter, composition of apoplast changed in ways that were distinct from the tissue. The concentrations of malate and K^+ increased markedly in apoplast samples taken during Stage II, as did the sum of apoplast solutes, all in contrast to the tissue. In PostV berries, much of the dramatic increase in total apoplastic solute was accounted for by fructose and glucose, but the concentrations of both were greater in tissue than in apoplast.

Table 2 Total soluble solids (TSS), mesocarp cell turgor pressure (P), tissue solute potential (Ψ_s^T), apoplast solute potential (Ψ_s^A) and the calculated solute potential, the measured solute potentials (Ψ_s) of berries sampled at three different developmental stages (Stage I, Stage II, and Stage III) for greenhouse-grown Chardonnay, and the measured solute potentials of model solutions reflecting the compositions in Fig. 6

Stage	TSS (°Brix)	P (MPa)	Ψ_s		Ψ_m [c] (MPa)	Calculated Ψ_s [d] (MPa)	Measured model solution Ψ_s [e] (MPa)
			Tissue (Ψ_s^T)[a] (MPa)	Apoplast (Ψ_s^A)[b] (MPa)			
Stage I	3.1 ± 0.1	0.25 ± 0.08	−0.75 ± 0.13	−0.23 ± 0.06	−0.27	−0.12 ± 0.04	−0.13 (56.5)[f]
Stage II	3.9 ± 0.2	0.29 ± 0.02	−0.86 ± 0.04	−0.69 ± 0.09	0.12	−0.45 ± 0.12	−0.46 (66.7)
Stage III	19.2 ± 1.2	0.06 ± 0.01	−3.48 ± 0.28	−3.37 ± 0.34	−0.05	−2.55 ± 0.34	−2.91 (86.4)

Data indicate Mean ± 1 SD

[a] Ψ_s^T indicates tissue solute potential from other berries for same clusters and is shown to compare with the data used for solutes assay

[b] Ψ_s^A indicates apoplast solute potential from other berries for same clusters and is shown to compare with the data used for solutes assay

[c] Ψ_m indicates the calculated matric potential (see Discussion)

[d] Calculated Ψ_s indicates total solute potential and was calculated from the total solutes concentration detected in Fig. 6 according to van't Hoff's equation at 37°C (310K)

[e] Each model solution was artificially prepared based on the averaged concentration of detected solutes (tartrate, malate, proline, fructose, glucose, sucrose and potassium), and the Ψ_s measured with the osmometer

[f] The contribution percentage of each model solution Ψ_s to the Ψ_s^A is given in parenthesis

We interpret these differences between apoplast and tissue solutes to indicate that the decreased Ψ_s^A and cell P is not caused by symplastic contamination from compartmentation breakdown (Lang and Düring 1991), but rather by the presence of regulated levels of solutes in the apoplast. The approximately 0.5 M accumulation of glucose and fructose in the PostV apoplast indicates that the decrease in Ψ_s^A is likely derived from inverted sucrose delivered in the phloem (Greenspan et al. 1994). Even though the compartmentation breakdown theory has gained some acceptance in grapes (Coombe 1992), it must be recognized that it is not based on any direct assays for cell P or membrane function. PostV mesocarp cells were found to have normal cell relaxation characteristics (Thomas et al. 2006) and positive P (Matthews and Shackel 2005; Thomas et al. 2006; present study). In addition, studies with the vital stain fluorescein diacetate (FDA) indicate viable cells well into fruit maturity (Krasnow et al. 2008). The compartmentation breakdown theory conflicts with accumulating evidence of ongoing cellular metabolism after veraison, such as upregulated expression of many genes including those for membrane intrinsic proteins, such as sugar transporters (Davies et al. 1999; Fillion et al. 1999) and aquaporins (Delrot et al. 2001; Picaud et al. 2003).

For PostV berries, a comparison of the theoretical contribution of all measured solutes ("Calculated" in Table 2) to the measured PostV Ψ_s^A revealed a difference of 0.82 MPa. For such concentrated solutions (PostV tissue reached c.a. −4.0 MPa), deviation from the ideality assumed in the van't Hoff relation may occur. We tested this by comparing the calculated Ψ_s to the measured Ψ_s of model solutions with the same composition used to obtain the calculated Ψ_s. The measured model solution Ψ_s for PreV (both Stage I and Stage II) was equivalent to the corresponding calculated Ψ_s, whereas the measured PostV model solution Ψ_s was 0.36 MPa more negative than the corresponding calculated Ψ_s. The direction of this discrepancy is consistent with that predicted by the theory of Cochrane (1994), with the calculated Ψ_s of 560 mM fructose, which was detected in the PostV apoplast, being −1.50 MPa at 20°C (Cochrane and Cochrane 2005), compared to the −1.37 MPa value calculated by the van't Hoff relation.

Solutes that were included in the model solution and measured, accounted for an increasing fraction of the Ψ_s^A during berry development. The contribution of the measured model solution Ψ_s to the Ψ_s^A increased from 56.5% in Stage I to 86.4% at 19 °Brix as the concentration of apoplastic carbohydrate became higher (Table 2). Hence, as the berries approached maturity only 13.6% of the Ψ_s^A remained undetected.

To complete an analysis of the role of Ψ_s^A, it is necessary to consider the apoplastic water relations of an individual cell. In general, total water potential (Ψ_w) of a cell is usually described as

$$\Psi_w = \Psi_s + P \quad (2)$$

where the Ψ_s can be equivalent to Ψ_s^T ($\approx \Psi_s$ in the mesocarp). By recognizing that the mesocarp cell forms two compartments separated by a plasma membrane, the water potential of the protoplast (Ψ_w^P) and apoplast (Ψ_w^A) in tissue can be described separately as,

$$\Psi_w^P = \Psi_s^P + P \quad (3)$$

$$\Psi_w^A = \Psi_s^A + \Psi_m \quad (4)$$

where Ψ_m is regarded as the tissue-averaged Ψ_m in the mesocarp apoplast. As described elsewhere (Nonami and

Boyer 1987; Boyer and Nonami 1990; Wada et al. 2005), the Ψ_w of the two compartments are locally equilibrated in the mesocarp, i.e., $\Psi_w^P \approx \Psi_w^A$. We measured the P, Ψ_s^T, and Ψ_s^A but not Ψ_m in the present work. However, by assuming that Ψ_s^P in Eq. (3) corresponds to Ψ_s^T, it is possible to estimate Ψ_m. Considering that mesocarp P was spatially uniform (Thomas et al. 2006), we estimate that the mesocarp-tissue averaged Ψ_w^A at Stage I, Stage II, and PostV was −0.50, −0.57 and −3.42 MPa, respectively. According to Eq. (4), the mesocarp tissue-averaged Ψ_m increased as the berry developed (Table 2), and the size of PostV Ψ_m is much smaller than that of PostV Ψ_s^A. Thus, the lowering of Ψ_s^A should make the total water potential lower, which is consistent with the observation of Matthews et al. (1987) that the berry (tissue-averaged) Ψ_w and tissue Ψ_s ($\approx \Psi_s^T$) begin to decrease dramatically before veraison. Similar results were also suggested with a pressure apparatus technique (Bondada et al. 2005). More recently, Zhang et al. (2006) reported that apoplastic solute concentration increased during PostV, although their concentrations (less than 200 mM) were much lower than our results, and too low to account for the several MPa lowering of Ψ_s^A measured here and of Ψ_w^A indicated in Matthews et al. (1987). Tyerman et al. (2004) modified a root pressure probe for measurement of berry hydraulics and found an increase in the equilibrium hydrostatic pressure in the berry pedicel near veraison, which is consistent with our calculations. If xylem tension is equilibrated with the Ψ_m in the mesocarp apoplast during PostV, then the size of xylem tension is also much smaller than Ψ_s^A.

It is important to keep in mind that P is influenced by the difference between Ψ_w^A and Ψ_s^P under near-equilibrium conditions. High concentrations of solute accumulate in the fruit, lowering the Ψ_w^A, and diminishing the Ψ_s gradient between apoplast and cell in the mesocarp tissue. This in turn probably regulates cell P, thus resulting in fruit softening. The apoplastic water relations reported here progressively changed during Stage II, prior to most of the physiological changes that are typically associated with the onset of ripening. Thus, we propose that the regulation of apoplastic solutes may be important as a regulatory event that leads to veraison.

Acknowledgments We thank Dr. Kentaro Inoue of the Department of Plant Sciences, University of California, Davis, for use of his centrifuge. We gratefully acknowledge Dr. Thomas T. Cochrane of Department of Civil Engineering, University of Canterbury, for providing us with his valuable data sheet for solute potential calculations. The authors also thank Cal-Western Nurseries, Visalia, CA, USA for providing Chardonnay grapevines.

References

Bernstein L (1971) Method for determining solutes in the cell walls of leaves. Plant Physiol 47:361–365

Bondada BR, Matthews MA, Shackel KA (2005) Functional xylem in the post-veraison grape berry. J Exp Bot 56:2949–2957

Boyer JS (1967) Leaf water potentials measured with a pressure chamber. Plant Physiol 42:133–137

Boyer JS, Nonami H (1990) Water potential and its components in growing tissues. In: Hashimoto Y, Kramer PJ, Nonami H, Strain BR (eds) Measurement techniques in plant science. Academic Press, San Diego, pp 101–112

Bruce DM (2003) Mathematical modelling of the cellular mechanics of plants. Philos Trans R Soc Lond B Biol Sci 358:1437–1444

Brummell DA, Harpster MH (2001) Cell wall metabolism in fruit softening and quality and its manipulation in transgenic plants. Plant Mol Biol 47:311–340

Cochrane TT (1994) A new equation for calculating osmotic potential. Plant Cell Environ 17:427–433

Cochrane TT, Cochrane TA (2005) Osmotic potential properties of solutes common in the soil-plant solution continuum. Soil Sci 170:433–444

Considine J, Brown K (1981) Physical aspects of fruit growth: theoretical analysis of distribution of surface growth forces in fruit in relation to cracking and splitting. Plant Physiol 68:371–376

Coombe BG (1976) Development of fleshy fruits. Annu Rev Plant Physiol Plant Mol Biol 27:207–228

Coombe BG (1992) Research on development and ripening of the grape berry. Am J Enol Vitic 43:101–110

Coombe BG, Bishop GR (1980) Development of the grape berry. II: Changes in diameter and deformability during veraison. Aust J Agri Res 31:499–509

Cosgrove DJ, Cleland RE (1983) Solutes in the free space of growing stem tissues. Plant Physiol 72:326–331

Dannel F, Pfeffer H, Marschner H (1995) Isolation of apoplasmic fluid from sunflower leaves and its use for studies on influence of nitrogen supply on apoplasmic pH. J Plant Physiol 146:273–278

Davies C, Wolf T, Robinson SP (1999) Three putative sucrose transporters are differentially expressed in grapevine tissues. Plant Sci 147:93–100

Delrot S, Picaud S, Gaudillere JP (2001) Water transport and aquaporins in grapevine. In: Roubelakis-Angelakis KA (ed) Molecular biology and biotechnology of the grapevine. Kluwer, London, pp 241–262

Fillion L, Ageorges A, Picaud S, Coutos-Thevenot P, Lemoine R, Romieu C, Delrot S (1999) Cloning and expression of a hexose transporter gene expressed during the ripening of grape berry. Plant Physiol 120:1083–1094

Greenspan MD, Shackel KA, Matthews MA (1994) Developmental changes in the diurnal water budget of the grape berry exposed to water deficits. Plant Cell Environ 17:811–820

Gutiérrez-Granda MJ, Morrison JC (1992) Solute distribution and malic enzyme activity in developing grape berries. Am J Enol Vitic 43:323–328

Hiwasa K, Nakano R, Hashimoto A, Matsuzaki M, Murayama H, Inaba A, Kubo Y (2004) European, Chinese and Japanese pear fruits exhibit differential softening characteristics during ripening. J Exp Bot 55:2281–2290

Hüsken D, Steudle E, Zimmermann U (1978) Pressure probe technique for measuring water relations of cells in higher plants. Plant Physiol 61:158–163

Jachetta JJ, Appleby AP, Boersma L (1986) Use of the pressure-vessel to measure concentrations of solutes in apoplastic and membrane-filtered symplastic sap in sunflower leaves. Plant Physiol 82:995–999

Krasnow MN, Matthews MA, Shackel KA (2008) Evidence for substantial maintenance of membrane integrity and cell viability in normally developing grape (*Vitis vinifera* L.) berries throughout development. J Exp Bot (in press)

Lang A, Düring H (1991) Partitioning control by water potential gradient: Evidence for compartmentation breakdown in grape berries. J Exp Bot 42:1117–1122

Lang A, Thorpe MR (1989) Xylem, phloem and transpiration flows in a grape: application of a technique for measuring the volume of attached fruits to high-resolution using Archimedes principle. J Exp Bot 40:1069–1078

Livingston DP, Henson CA (1998) Apoplastic sugars, fructans, fructan exohydrolase, and invertase in winter oat: responses to second-phase cold hardening. Plant Physiol 116:403–408

Lohaus G, Pennewiss K, Sattelmacher B, Hussmann M, Muehling KH (2001) Is the infiltration–centrifugation technique appropriate for the isolation of apoplastic fluid?: a critical evaluation with different plant species. Physiol Plant 111:457–465

Matthews MA, Shackel KA (2005) Growth and water transport in fleshy fruit. In: Holbrook MN, Zwieniecki MA (eds) Vascular transport in plants. Elsevier, Boston, pp 189–197

Matthews MA, Anderson MM (1988) Fruit ripening in *Vitis vinifera* L.: responses to seasonal water deficits. Am J Enol Vitic 39:313–320

Matthews MA, Cheng G, Weinbaum SA (1987) Changes in water potential and dermal extensibility during grape berry development. J Am Soc Hort Sci 112:314–319

Meinzer FC, Moore PH (1988) Effect of apoplastic solutes on water potential in elongating sugarcane leaves. Plant Physiol 86:873–879

Mignani I, Greve LC, Benarie R, Stotz HU, Li CY, Shackel KA, Labavitch JM (1995) The effects of GA_3 and divalent-cations on aspects of pectin metabolism and tissue softening in ripening tomato pericarp. Physiol Plant 93:108–115

Nonami H, Boyer JS (1987) Origin of growth-induced water potential: solute concentration is low in apoplast of enlarging tissues. Plant Physiol 83:596–601

Ogden TE, Citron MC, Pierantoni R (1978) The jet stream microbeveler: an inexpensive way to bevel ultrafine glass micropipettes. Science 201:469–470

Picaud S, Becq F, Dedaldechamp F, Ageorges A, Delrot S (2003) Cloning and expression of two plasma membrane aquaporins expressed during the ripening of grape berry. Funct Plant Biol 30:621–630

Pomper KW, Breen PJ (1995) Levels of apoplastic solutes in developing strawberry fruit. J Exp Bot 46:743–752

Rose JKC, Lee HH, Bennett AB (1997) Expression of a divergent expansin gene is fruit-specific and ripening-regulated. Proc Natl Acad Sci USA 94:5955–5960

Sakurai N (1998) Dynamic function and regulation of apoplast in the plant body. J Plant Res 111:133–148

Saladié M, Matas AJ, Isaacson T, Jenks MA, Goodwin SM, Niklas KJ, Ren XL, Labavitch JM, Shackel KA, Fernie AR, Lytovchenko A, O'Neill MA, Watkins CB, Rose JKC (2007) A reevaluation of the key factors that influence tomato fruit softening and integrity. Plant Physiol 144:1012–1028

Shackel KA, Greve C, Labavitch JM, Ahmadi H (1991) Cell turgor changes associated with ripening in tomato pericarp tissue. Plant Physiol 97:814–816

Shackel KA, Matthews MA, Morrison JC (1987) Dynamic relation between expansion and cellular turgor in growing grape (*Vitis vinifera* L.) leaves. Plant Physiol 84:1166–1171

Soga T, Imaizumi M (2001) Capillary electrophoresis method for the analysis of inorganic anions, organic acids, amino acids, nucleotides, carbohydrates and other anionic compounds. Electrophoresis 22:3418–3425

Speer M, Kaiser WM (1991) Ion relations of symplastic and apoplastic space in leaves from *Spinacia oleracea* L. and *Pisum sativum* L. under salinity. Plant Physiol 97:990–997

Tang AC, Boyer JS (2002) Growth-induced water potentials and the growth of maize leaves. J Exp Bot 53:489–503

Terry ME, Bonner BA (1980) An examination of centrifugation as a method of extracting an extracellular solution from peas, and its use for the study of indoleacetic acid-induced growth. Plant Physiol 66:321–325

Tetlow IJ, Farrar JF (1993) Apoplastic sugar concentration and pH in barley leaves infected with brown rust. J Exp Bot 44:929–936

Thomas TR (2004) Grape berry cellular turgor: responses to water deficits, relation to fruit firmness, and changes throughout development in Cabernet Sauvignon, Chardonnay, and Pinot noir. MS thesis, University of California, Davis

Thomas TR, Matthews MA, Shackel KA (2006) Direct in situ measurement of cell turgor in grape (*Vitis vinifera* L.) berries during development and in response to plant water deficits. Plant Cell Environ 29:993–1001

Tong C, Krueger D, Vickers Z, Bedford D, Luby J, El-Shiekh A, Shackel K, Ahmadi H (1999) Comparison of softening-related changes during storage of 'Honeycrisp' apple, its parents, and 'Delicious'. J Am Soc Hort Sci 124:407–415

Tyerman SD, Tilbrook J, Pardo C, Kotula L, Sullivan W, Steudle E (2004) Direct measurement of hydraulic properties in developing berries of *Vitis vinifera* L. cv Shiraz and Chardonnay. Aust J Grape Wine Res 10:170–181

Wada H, Iwaya-Inoue M, Akita M, Nonami H (2005) Hydraulic conductance in tepal growth and extension of vase life with trehalose in cut tulip flowers. J Am Soc Hort Sci 130:275–286

Wakabayashi K (2000) Changes in cell wall polysaccharides during fruit ripening. J Plant Res 113:231–237

Welbaum GE, Meinzer FC (1990) Compartmentation of solutes and water in developing sugarcane stalk tissue. Plant Physiol 93:1147–1153

Yu Q, Tang C, Kuo J (2000) A critical review on methods to measure apoplastic pH in plants. Plant Soil 219:29–40

Zhang WH, Atwell BJ, Patrick JW, Walker NA (1996) Turgor-dependent efflux of assimilates from coats of developing seed of *Phaseolus vulgaris* L.: water relations of the cells involved in efflux. Planta 199:25–33

Zhang XY, Wang XL, Wang XF, Xia GH, Pan QH, Fan RC, Wu FQ, Yu XC, Zhang DP (2006) A shift of phloem unloading from symplasmic to apoplasmic pathway is involved in developmental onset of ripening in grape berry. Plant Physiol 142:220–232

Zhu J, Chen S, Alvarez S, Asirvatham VS, Schachtman DP, Wu Y, Sharp RE (2006) Cell wall proteome in the maize primary root elongation zone. I. Extraction and identification of water-soluble and lightly ionically bound proteins. Plant Physiol 140:311–325